Holey random walks: Optics of heterogeneous turbid composites

Tomas Svensson,[1,*] Kevin Vynck,[1,†] Marco Grisi,[1,‡] Romolo Savo,[1] Matteo Burresi,[1,2] and Diederik S. Wiersma[1,2]
[1]*European Laboratory for Non-Linear Spectroscopy, University of Florence, Via Nello Carrara 1, 50019 Sesto Fiorentino, Firenze, Italy*
[2]*Istituto Nazionale di Ottica, Consiglio Nazionale delle Ricerche, Largo Fermi 6, 50125 Firenze, Firenze, Italy*
(Received 13 November 2012; published 15 February 2013)

We present a probabilistic theory of random walks in turbid media with nonscattering regions. It is shown that important characteristics such as diffusion constants, average step lengths, crossing statistics, and void spacings can be analytically predicted. The theory is validated using Monte Carlo simulations of light transport in heterogeneous systems in the form of random sphere packings and good agreement is found. The role of step correlations is discussed and differences between unbounded and bounded systems are investigated. Our results are relevant to the optics of heterogeneous systems in general and represent an important step forward in the understanding of media with strong (fractal) heterogeneity in particular.

DOI: 10.1103/PhysRevE.87.022120 PACS number(s): 05.40.Fb, 42.25.Dd, 42.68.Ay, 05.10.Ln

I. INTRODUCTION

Multiple scattering of light is ubiquitous in nature and a proper account of the phenomenon is essential in important areas such as atmospheric science [1–3], biomedical optics [4–6], and material characterization [7–10]. The transport of light in turbid media is typically treated within the framework of classical radiative transfer, i.e., as a Poissonian random walk of independent and exponentially distributed ballistic segments (steps) (see Refs. [2,5,11]). For optically thick samples, i.e., on scales over which light experiences a large number of scattering events, macroscopic transport is well described by a diffusion equation with a simple expression for the diffusion constant $D = v\ell/3$, where v is the energy velocity and ℓ the mean step length [12–14]. It is important to realize that this widely used expression is intimately linked with the assumption of a *uniform* (random) distribution of scatterers that yields exponentially distributed random steps. However, there is an abundance of real turbid systems in which scatterers are *not* uniformly distributed. In such systems, the distribution of step lengths between successive scattering events is no longer exponential and, due to quenched disorder (i.e., a frozen geometry), correlations between these steps can be significant. This invalidates the above given expression for D. As it has become better understood that the presence of inhomogeneities has important implications in a wide variety of contexts, from the optics of cloudy atmospheres [3,15–17] to spectroscopy of the human body [18–26] and transport in colloids, porous media, and foams [27–31], this matter calls for attention.

Deviations from the homogenized viewpoint can be particularly important for strongly heterogeneous systems that are characterized by, or can be modeled as, a turbid medium with embedded nonscattering regions of significant size. Here clouds are an important example [15,16,32]. The interest in systems with nonscattering regions has been increased further by the recent fundamental studies of superdiffusion of light in disordered materials with an engineered *fractal* heterogeneity (i.e., nonscattering regions of sizes ranging over several orders of magnitude), dubbed Lévy glasses [33,34], in which transport relies on an interplay between a broad step length distribution and quenched disorder [35–37]. Yet another example of turbid systems with holes is complex porous media, where broad pore size distributions can influence light diffusion [29].

Unfortunately, since light transport in heterogeneous systems is intrinsically dependent on the specific heterogeneity, its description in general terms is particularly challenging. Significant effort has been devoted to the non-Poissonian transport mechanisms appearing in heterogeneous systems, mainly by finding new ways to homogenize the medium and setting up generalized transport equations [32,38–44]. However, little is known about light transport in turbid media with quenched disorder in the form of nonscattering regions. Interestingly, the problem of how nonscattering regions impact transport in scattering media has been studied in the specific context of neutron diffusion in pebble bed reactors [45,46]. Therein a rather intricate expression of the modified diffusion constant has been derived, neglecting step correlations and being applied essentially to weakly scattering media containing monodisperse scattering volumes or holes. A theoretical study of transport in strongly heterogeneous media in general (i.e., including polydispersive and fractal-like media), which provides physical insight into the modification of the diffusion process, the onset of diffusion at early times, the importance of step correlations, and the impact of finite system size on transport, is however still missing. The main purpose of this work is to address this issue.

In this article we present a probabilistic theory of light transport in turbid media containing nonscattering regions. Addressing both monodispersive and polydispersive systems, we show that important quantities such as asymptotic diffusion constants, step length distributions, and void crossing statistics can be analytically predicted via remarkably simple and intuitive formulas. The success of the theoretical approach is verified by an extensive analysis of random walks in disordered three-dimensional polydispersive sphere packings (the intersphere volume is set to be homogeneously turbid). Our findings provide important insight into light transport in materials with spatial heterogeneity in scatterer density, including porous materials and disordered optical materials

*svensson@lens.unifi.it
†Present address: Institut Langevin, ESPCI ParisTech, 1 rue Jussieu, 75005 Paris, France.
‡Present address: Swiss Federal Institute of Technology of Lausanne (EPFL), Switzerland.

with engineered fractal heterogeneity, such as Lévy glasses [33–37,47,48].

The remainder of the paper is organized as follows. The analytical approach for holey random walks is presented in Sec. II. Based on equilibrium considerations, we show that the mean step length equals that of a homogenized system. Using an analytical model for the spacing between spheres in random sphere packings, we derive an analytical expression for the diffusion constant, as modified by the presence of holes in the system. In Sec. III we perform an extensive study of multiple scattering in holey systems formed by monodispersive and polydispersive sphere packings (from the weakly to the strongly scattering regime) to check the validity of the derived diffusion constant and multisphere crossing probabilities. The evolution of the mean-square displacement is used to study the onset of diffusion and the role of step correlations is investigated and discussed. We also investigate finite-size effects on transport in turbid media with fractal heterogeneity (Lévy glasses), showing that they cannot be described by normal diffusion. A summary is given in Sec. IV.

II. ANALYTICAL DESCRIPTION OF HOLEY RANDOM WALKS

Let us consider the general case of a random walk in a composite medium consisting of arbitrarily shaped nonscattering regions embedded in a turbid medium (a holey system), the void filling fraction being ϕ (see Fig. 1). We will assume that isotropic scatterers are randomly distributed in the turbid medium, meaning that the distance between isotropic scattering events is exponentially distributed with a scattering mean free path ℓ_s. The scattering mean free path is related to single-scattering properties via

$$\ell_s = \frac{1}{n\sigma_s}, \tag{1}$$

where n denotes the number density of scatterers and σ_s the scattering cross section. In general, the random step length S between two subsequent scattering events in the composite heterogeneous medium consists of two parts: a length $S_{\text{turbid}} \in \exp(\ell_s)$ inside the turbid intervoid medium and a length S_{void} inside nonscattering voids:

$$S = S_{\text{turbid}} + S_{\text{void}}. \tag{2}$$

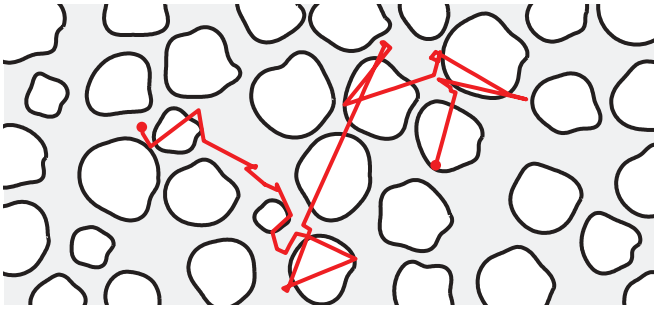

FIG. 1. (Color online) Holey random walk. Random walkers change direction randomly in time, but only when traveling in the turbid medium found in between the nonscattering regions (holes). Transport is governed by the resulting step length distribution and step correlations in a complex manner.

Here it should be noted that S_{turbid} and S_{void} are not independent random variables. On the contrary, they are positively correlated: A long step in the turbid medium is more likely to be accompanied by one or several crossings of nonscattering regions.

A. Equilibrium considerations

Assuming that the density of states is homogeneous (which in optics corresponds to a constant refractive index), random walkers at equilibrium should sample the two constituents according to their respective volume fraction. We then expect that a fraction ϕ of the average step is located to voids, i.e.,

$$E[S_{\text{void}}] = \phi E[S], \tag{3}$$

$$E[S_{\text{turbid}}] = (1-\phi)E[S]. \tag{4}$$

In terms of expectations values we have

$$E[S] = E[S_{\text{void}}] + E[S_{\text{turbid}}]; \tag{5}$$

using that we also know by definition that $E[S_{\text{turbid}}] = \ell_s$, we reach $E[S] = \phi E[S] + \ell_s$ and conclude that

$$E[S] = \frac{\ell_s}{1-\phi} = \ell_h. \tag{6}$$

This important result that tells us two things: The mean step length is independent of the shape and size distribution of the nonscattering regions and equals the homogenized scattering mean free path ℓ_h that would govern a system where the scatterers were randomly distributed over the full volume instead of only a volume fraction $1-\phi$ [n going from n_0 to $n_0(1-\phi)$ in Eq. (1)]. Thus $E[S]$ is dependent only on ϕ, not on the sizes of the voids. This means that the mean step will grow only with an increase of ϕ and not with the inclusion of increasingly larger voids.

B. General remark regarding diffusion

Although the mean step is a very important quantity, transport properties are determined by the step length distribution as a whole. In particular, when steps can be considered independent, the diffusion constant that governs the macroscopic spreading of random walkers is determined by the ratio of the first two moments of the step distribution (when finite). This important relation can easily be derived by considering the summation of independent d-dimensional isotropic random steps, all following the same (arbitrary) step length distribution. One finds that the mean-square displacement asymptotically grows as $2dDt$ with a diffusion constant D given by

$$D = \frac{1}{2d} v \frac{E[S^2]}{E[S]}, \tag{7}$$

where S denotes the scalar length (norm) of the individual steps and v is the walk velocity. For purely exponential steps in three dimensions, corresponding to a homogenous distribution of isotropic scatterers, this expression reduces to the famous relation

$$D = \tfrac{1}{3} v \ell, \tag{8}$$

where ℓ is the mean length of the exponential steps. It should be noted that this relation is normally derived via the radiative transfer equation [13,49], not by considering the summation of random variables (however, see, e.g., Refs. [50,51] for similar considerations). For a general holey system, with heterogeneous distribution of scatterers, steps are not exponential distributed and the simple formula of Eq. (8) does not hold. Interestingly, we have already shown that the mean step length $E[S]$ of the holey system is independent of the scatterer distribution. The second moment $E[S^2]$, in contrast, will depend on the particular heterogeneity and scatterer density in a complex manner.

C. Sphere packings as holey systems

As indicated above, transport in a general holey system is complicated. Besides the issue of step length distribution, step correlations may be important and must not be forgotten. To gain insight into this complicated matter we will turn to systems where the nonscattering part of the system has the form of a polydispersive random sphere packing. In this and the following section, we will present an analytical theory of transport in such systems. In subsequent sections, this theory will be compared to Monte Carlo simulations of random walks in sphere-packing realizations.

Let r_i $(i = 1, \ldots, M)$ denote the different radii of the involved spheres and n_i their respective number densities. A random walker traveling in this system will scatter randomly in time, but only when outside the nonscattering regions. While being scattered, the chance of crossing at least one sphere in the coming step depends on the probability that the next step is longer than the distance to the next sphere surface (along the new walker direction). This distance can be seen as a random variable and is here denoted Δ_{ps} (point-sphere spacing). If a sphere is crossed, the probability of crossing also a second sphere before being scattered now depends on the sphere-sphere spacing along the direction of the walker. This distance also is a random variable and we denote it Δ_{ss} (sphere-sphere spacing). The actual step length distribution will be determined by the distributions of these random variables (of course, in combination with the intersphere scattering mean free path ℓ_s). Figure 2 illustrates the definition of these two essential distance variables.

The average spacing between spheres Δ_{ss}, as experienced by the random walker, can be analytically calculated from the filling fraction and the sphere distribution. If we consider a random line drawn through the sphere packing, it is evident that a fraction $1 - \phi$ of it will be drawn through the intersphere medium. Letting $E[\zeta]$ denote the average length of the individual chords through the spheres, we have that

$$\frac{E[\Delta_{\mathrm{ss}}]}{E[\Delta_{\mathrm{ss}}] + E[\zeta]} = 1 - \phi \tag{9}$$

and, similarly to Olson *et al.* [52], conclude that

$$E[\Delta_{\mathrm{ss}}] = \frac{1-\phi}{\phi} E[\zeta]. \tag{10}$$

The average chord length $E[\zeta]$ can in turn be calculated from the sphere distribution. Let p_i denote the probability that a random chord is made in a sphere of radius r_i. Intuitively, this probability should be proportional to the total surface area of the sphere category, i.e.,

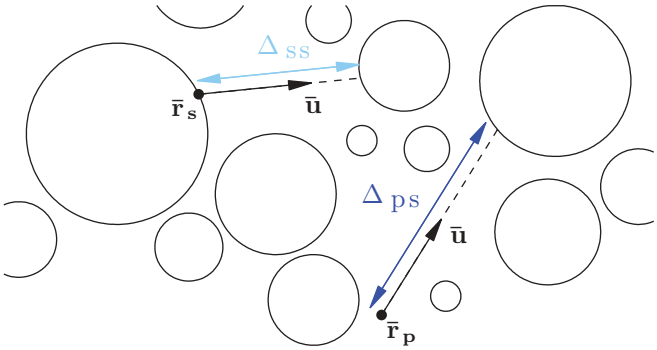

FIG. 2. (Color online) From a random-walk perspective, two central characteristics of the sphere packing are the distribution of the (i) distance from a random point $\bar{\mathbf{r}}_{\mathbf{p}}$ (scattering event) along a random direction $\bar{\mathbf{u}}$ to a sphere surface $\Delta_{\mathrm{ps}}(\bar{\mathbf{r}}_{\mathbf{p}}, \bar{\mathbf{u}})$ and (ii) distance to the next sphere along a random direction when leaving a sphere at a random point $\bar{\mathbf{r}}_{\mathbf{s}}$, $\Delta_{\mathrm{ss}}(\bar{\mathbf{r}}_{\mathbf{s}}, \bar{\mathbf{u}})$. Their distributions can be assessed via statistical analysis of sphere packings. Later we show that the mean value of Δ_{ss}, as experienced by the random walker, can be analytically predicted.

$$p_i = \frac{A_i}{\sum_j A_j} = \frac{n_i r_i^2}{\sum_j n_j r_j^2}. \tag{11}$$

In fact, this view is equivalent to the equilibrium argument adhered to in this article: The total path made through the different sphere categories should equal their fraction of the total volume. Assuming an isotropic flux of random walkers close to the sphere surfaces (see the discussion in Ref. [53]), the length of a chord through a sphere of radius r_i follows a triangular probability density function $f_i(x) = x/2r_i^2$ in $0 \leqslant x \leqslant 2r_i$. The average chord is $\ell_i = 4r_i/3$ and the mean-square chord is $2r_i^2$. The probability density function of a random chord ζ in the polydispersive packing $f_\zeta(x)$ is a weighted sum of the individual chord distributions f_i:

$$f_\zeta(x) = \sum_i p_i f_i(x) = \sum_{i:2r_i > x} p_i \frac{x}{2r_i^2}. \tag{12}$$

The mean overall chord then becomes

$$E[\zeta] = \sum p_i \ell_i = \sum p_i \frac{4r_i}{3} \tag{13}$$

and its mean square

$$E[\zeta^2] = \sum p_i 2r_i^2. \tag{14}$$

D. Exponential spacing model

From statistical analysis of random sphere packings, we generally find that $E[\Delta_{\mathrm{ps}}] \approx E[\Delta_{\mathrm{ss}}]$ and distributions have near-exponential decay. We therefore propose a model in which the actual (complicated) distributions of Δ_{ps} and Δ_{ss} are modeled with a *single* exponentially distributed random spacing Δ with mean spacing $\bar{\Delta}$, i.e., $\Delta \in \exp(\bar{\Delta})$. In fact, it has been shown that spacing between random objects is, to a very good approximation, exponential at low filling fractions [52]. At higher filling fractions, spacing distributions

are no longer perfectly exponential, but rather a complicated function of the exact structure [52,54,55]. However, also in such cases we will show that the errors due to the use of a simple exponential spacing model can be reasonably small.

Within the exponential spacing model, the probability that an exponentially distributed step $S_{\text{turbid}} \in \exp(l_s)$ will not take the random walker to a sphere is

$$P_0 = P(S_{\text{turbid}} < \Delta) = \frac{\bar{\Delta}}{\bar{\Delta} + \ell_s}. \tag{15}$$

Given the memoryless property of the Poisson process that governs scattering events, the number of crossings naturally follows a geometric distribution. This means that the probability of crossing n spheres between two scattering events is

$$P_n = (1 - P_0)^n P_0. \tag{16}$$

The average number of sphere crossings per step N is, within this model,

$$E[N] = \sum n P_n = \frac{1 - P_0}{P_0} = \frac{\ell_s}{\bar{\Delta}}. \tag{17}$$

In order to fulfill the equilibrium condition, $\bar{\Delta}$ must be chosen so that the average step samples the medium according to volume fractions. Assuming that the numbers of sphere crossings and involved chord lengths are independent, we should have that

$$\frac{E[N]E[\zeta]}{E[N]E[\zeta] + \ell_s} = \phi. \tag{18}$$

Using Eq. (17), we then reach the conclusion that

$$\bar{\Delta} = E[\Delta_{\text{ss}}] = \frac{1 - \phi}{\phi} E[\zeta]. \tag{19}$$

The exponential spacing model we have now outlined allows us to the estimate the step length distribution. In particular we can use it to estimate the mean-square step $E[S^2]$. Again, we will assume that for each step, the involved chord lengths are independent of the number of sphere crossings. By splitting the outcome of S^2 into the number of crossings and summing the conditional expectations (details in Appendix A) we find that

$$\begin{aligned} E[S^2] &= E\left[S_{\text{turbid}}^2\right] + E\left[S_{\text{void}}^2\right] + 2E[S_{\text{turbid}} S_{\text{void}}] \\ &= 2\ell_s^2 + \sum_{n=0}^{\infty} P_n \{n E[\zeta^2] + n(n-1) E[\zeta]^2\} \\ &\quad + 2 \sum_{i=0}^{\infty} P_n n E[\zeta](n+1) \frac{\bar{\Delta}\ell_s}{\bar{\Delta} + \ell_s} \\ &= 2\ell_h^2 + \phi \ell_h \frac{E[\zeta^2]}{E[\zeta]}. \end{aligned} \tag{20}$$

E. Diffusion constant for a holey system

Assuming that step correlations are negligible and remembering that $E[S] = \ell_h$, the expression for $E[S^2]$ given above [Eq. (20)] allows us to write a closed-form expression for the diffusion constant that governs macroscopic transport. Introducing the homogenized diffusion constant

$$D_h = \tfrac{1}{3} v \ell_h \tag{21}$$

and the chord-domain diffusion constant (the diffusion constant for a random walk with steps purely following the chord step distribution)

$$D_\zeta = \frac{1}{6} v \frac{E[\zeta^2]}{E[\zeta]}, \tag{22}$$

we reach, via Eq. (7), the surprisingly simple relation

$$D = D_h + \phi D_\zeta. \tag{23}$$

Interestingly, the diffusion constant of the heterogeneous system is given by the homogenized diffusion constant plus a term that is independent of the intervoid scattering mean free path ℓ_s. Note also that, as expected, the expression reduces to the homogenized diffusion constant as ϕ approaches zero.

III. MONTE CARLO SIMULATIONS OF TRANSPORT IN QUENCHED DISORDER

To illustrate the validity and importance of the theory presented in the preceding sections, this section will compare it with Monte Carlo (MC) simulations of transport in quenched random sphere packings. We use the term *quenched* to emphasize that the random walk is done in the quenched (frozen) heterogeneity of a random sphere packing and not in the fully annealed disorder model. The sphere packings used in our simulations are created by the random sequential addition of spheres [56] in descending order of size. Moreover, they are created to have periodic boundary conditions, i.e., so that the complete (cubic) sphere packing can act as a unit cell that can be stacked in all directions. As illustrated in Fig. 3, random walks are performed so that when crossing a boundary of the unit cell, the random walk can be continue on the opposite side of the same unit cell (while keeping track of unit cell coordinates). The use of periodic boundary conditions in this manner allows us to use realistic sizes of sphere packings and still being able to track walkers for long times and average dynamics over local disorder realization in an efficient way. Still, the size of the unit cell is made large enough to render the effects of periodicity negligible (the sizes of utilized sphere packings are carefully stated). We base our investigations on equilibrium starting conditions, i.e., allowing walkers to start randomly over the whole unit cell (including the interior of the nonscattering regions). For step statistics, only full steps between scattering events are considered. To be on the optical time scale, walkers are set to travel at a speed of $v = 200$ μm/ps (corresponding to a refractive index of 1.5).

A. Monodisperse sphere packing

The first case study is a holey system based on a monodispersive sphere packing. The nonscattering part of the material is composed of randomly placed spheres of radius 50 μm, the sphere filling fraction being $\phi = 0.3$. Figure 4 exemplifies the mean-square displacement obtained by averaging the dynamics of 5×10^5 random walkers launched randomly in a cubic system with a side of about 12 mm (10^6 randomly placed spheres). The average spacing between spheres is, in this case, 155.6 μm [as given by Eq. (10)]. As discussed in the

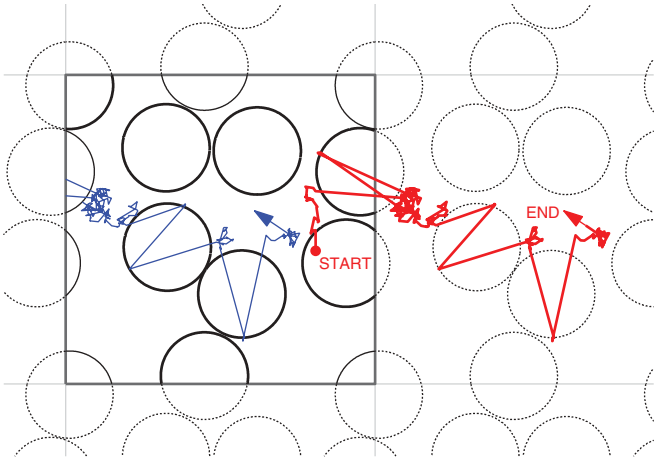

FIG. 3. (Color online) Two-dimensional illustration of unbounded holey random walks based on a sphere packing with periodic boundary conditions. When a walker leaves the sphere packing unit cell (marked square), the walk continues on the opposite side of the same sphere packing. The path of interest (red path, partly outside the unit cell) is reconstructed by keeping track of boundary crossings, but the path outside the unit cell is in reality a path inside the only unit cell (blue path). The use of periodic boundary conditions in this manner enables the use of realistically sized sphere packings, efficient averaging over disorder realization by allowing walkers to start also close to the sphere-packing boundaries, and long-time tracking of spreading. At the same time, the size of the unit cell is made large enough to render the effects of periodicity negligible.

figure caption, the outcome is in excellent agreement with our theory.

The applicability of our theory is further elaborated in Fig. 5, in which we study how the diffusion constant depends on the intersphere scattering mean free path ℓ_s. Interestingly, the example shows that even for cases where the average spacing between spheres $E[\Delta_{ss}]$ is several times larger than ℓ_s, step correlations are negligible and our analytical theory is applicable. Of course, when ℓ_s becomes significantly smaller than the void size, the increase in return probabilities should affect transport (steps become anticorrelated). This is in good agreement with the result that step correlations in this monodispersive system are important only for $\ell_s < r/2 = 25\ \mu$m. The strong quenching regime requires separate treatment and is beyond the scope of this article.

B. Fractal sphere packing

Let us now turn to the more general case of a polydispersive sphere packing, i.e., a situation where the nonscattering regions vary in size. We study the limiting case of a system with fractal heterogeneity (over two orders of magnitude) and a high sphere filling fraction. More specifically, our sphere packing is based on $M = 18$ sphere categories where the radii r_i are sampled exponentially from $r_{\min} = 2.5\ \mu$m up to $r_{\max} = 200\ \mu$m, i.e.,

$$r_i = r_{\min} \exp\left[\ln\left(\frac{r_{\max}}{r_{\min}}\right) \frac{i-1}{M-1} \right]. \qquad (24)$$

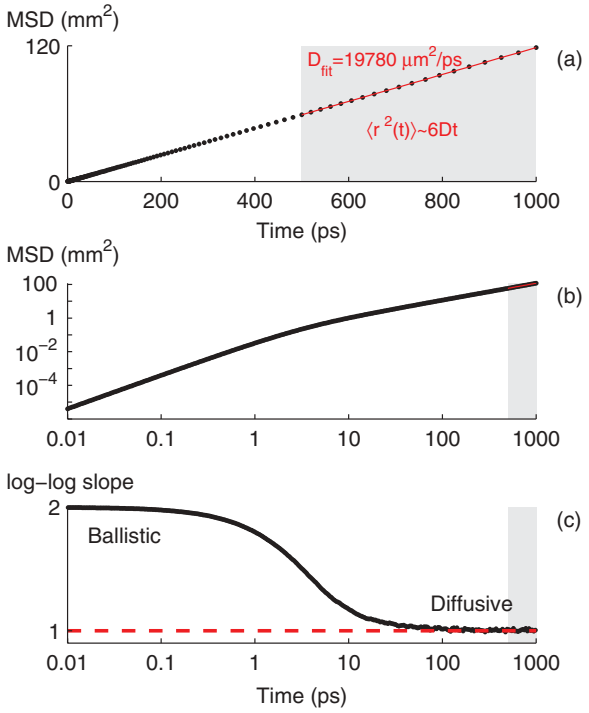

FIG. 4. (Color online) Dynamics for a holey system based on a monodispersive sphere packing ($r = 50\ \mu$m, $\phi = 0.3$, $\ell_s = 200\ \mu$m, and $v = 200\ \mu$m/ps). The diffusion constant extracted from analysis of the MSD evolution is in excellent agreement with the diffusion constant predicted by our theory [Eq. (23)]. For this system theory predicts a diffusion constant of 19 798 μm^2/ps and a linear fit over the temporal range indicated in gray in (a) gave 19 780 $\pm$ 34 μm^2/ps (mean $\pm$ standard error of the mean, as obtained from five simulation repetitions with 10^5 random walkers each). The middle graph (b) shows a log-log plot of (a). By showing the slope of the log-log plot, the bottom graph (c) reveals the transition from ballistic to diffusive dynamics and verifies that the temporal range used in our analysis falls within the asymptotic diffusive limit.

The number density of the spheres is set proportional to $1/r_i^3$ (i.e., the different sphere categories all occupy the same volume fraction) and the filling fraction of the system as a whole is $\phi = 0.7005$ (9 507 676 spheres in a cube with a side of about 2 mm).

Figure 6 highlights the success of the exponential spacing model also for such a complex heterogeneous system. In particular, this means that we have good quantitative knowledge about the step length distribution (including the sphere crossing statistics).

Using $\ell_s = \bar{\Delta}$ as a first test case, Fig. 7 shows the onset of diffusion and the asymptotic diffusion constant. Interestingly, the asymptotic diffusion constant is in this case about 25% lower than what we would have if steps were independent. With decreasing scattering strength, the importance of step correlations steadily decreases and the diffusion constant becomes in good agreement with our analytical expression $D = D_h + \phi D_\zeta$. This behavior is illustrated in Fig. 8, which shows simulations for ℓ_s being 1 to 8 times $\bar{\Delta}$. In this context, we want to emphasize that step correlations *per se* do not affect the applicability of the exponential spacing model and the accuracy of the related $E[S^2]$ estimation [Eq. (20)]. Instead,

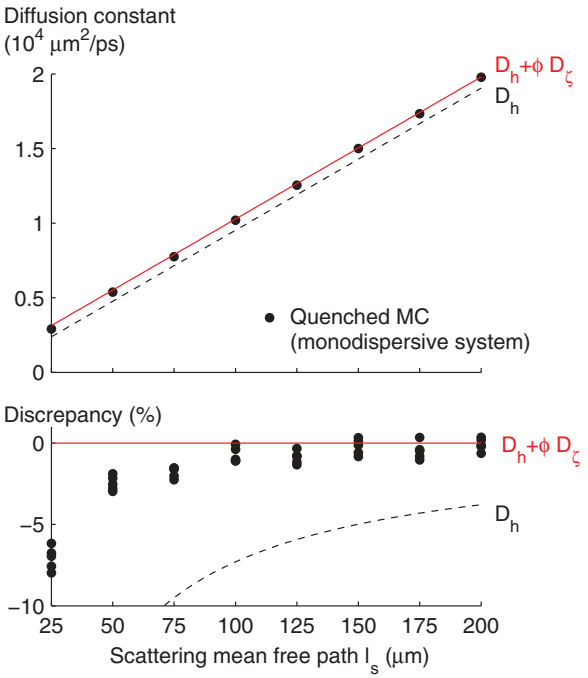

FIG. 5. (Color online) The analytical theory for the diffusion constant [red solid line, Eq. (23)] is in excellent agreement with the quenched Monte Carlo simulation of transport in a monodispersive sphere packing with $r = 50\ \mu$m and $\phi = 0.3$ (solid dots, average of five repetitions of 10^5 walkers per level of ℓ_s). This graph shows how D obtained from simulations exceeds the homogenized diffusion constant D_h (dashed line) exactly by the amount ϕD_ζ, largely independent of ℓ_s. As scattering becomes stronger and stronger (reduction in ℓ_s), anticorrelations between steps should reduce D and deviations from our theory are expected. The bottom graph clarifies that, in this particular case, this effect becomes important only for ℓ_s smaller than approximately $r/2 = 25\ \mu$m (here all five repetitions are shown). Note that the mean spacing between spheres is $E[\Delta_{ss}] \approx 156\ \mu$m.

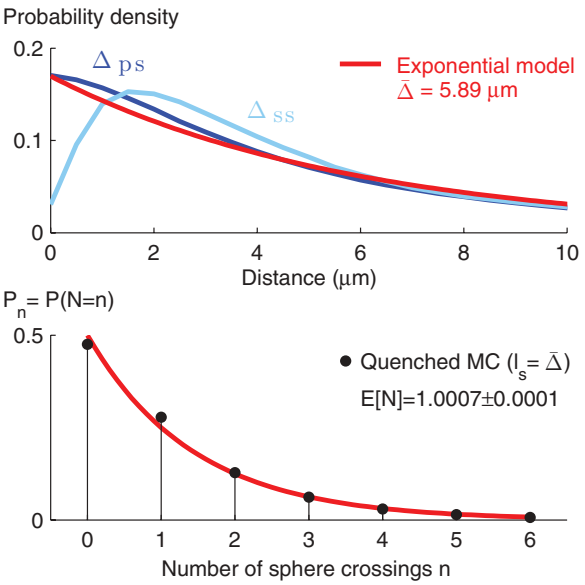

FIG. 6. (Color online) The theoretical predictions of the exponential spacing model are in good agreement with both quenched simulations and statistical analysis of a strongly polydispersive sphere packing. The success is illustrated here for the case of a fractal sphere packing with $M = 18$ radius categories ranging from $r_{min} = 2.5\ \mu$m to $r_{max} = 200\ \mu$m (9 507 676 spheres in a cube with a side of about 2 mm, $\phi = 0.7005$). As shown in the top graph, the analytically predicted mean spacing of $\bar{\Delta} = 5.89\ \mu$m is in good agreement with spacing distributions obtained via statistical analysis of the sphere packing ($E[\Delta_{ps}] \approx E[\Delta_{ss}] \approx 6\ \mu$m). The bottom graph highlights that the crossing probabilities P_n predicted by the exponential spacing model [Eq. (16)] agree almost perfectly with simulations running at $\ell_s = \bar{\Delta}$. In particular, setting $\ell_s = \bar{\Delta}$ (as done in this simulation) clearly renders $E[N] = 1$. The mean and mean-square steps are also in good agreement with theory. Theory predicts $E[S] = \ell_h = 19.669\ \mu$m and $E[S^2] = 1776.7\ \mu$m^2 and simulations give $19.679 \pm 0.004\ \mu$m and $1692 \pm 1\ \mu$m^2, respectively (mean $\pm$ standard error). That the observed mean-square step is a few percent lower than the theoretical prediction is consistent with the fact that the exponential model slightly overestimates the number of higher-order multicrossings ($n \geqslant 3$). This in turn can be understood by looking at the top graph and noting that the sphere-sphere spacing distance often will be underestimated by the exponential spacing model.

they only affect the validity of the assumption of independent steps that leads to $D = D_h + \phi D_\zeta$ [Eq. (23)].

Before ending this section we make a brief comparison to the monodispersive system studied in the preceding section. There we found that step anticorrelations started to play a role only when the scattering mean free path was smaller than the size of the involved spheres. For our polydispersive system, the situation is more complicated. The average spacing between spheres is only a few micrometers and the sphere sizes range from 5 to 400 μm. One can expect that large spheres will give rise to strong step anticorrelations, but since the transport between these larger spheres is a complicated function also of the smaller spheres in between, it is difficult to know for which ℓ_s this effect becomes important. As shown in Fig. 8, step correlation is of little important once ℓ_s is larger than, say, $4\bar{\Delta} \approx 25\ \mu$m. As mentioned also in the figure caption, this scattering strength gives a mean step $E[S] = \ell_h$ of about 80 μm. That correlations are weak can then be (partly) understood by realizing that most spheres are significantly smaller than this mean step length (the mean chord of the system is in fact not longer than $E[\zeta] = 13.8\ \mu$m).

C. Finite-size fractal sphere packings: Lévy glass

So far we have investigated unbounded holey systems. In practice, one often deals with a finite-size system where transport can be even more complicated to understand. For homogeneous media, for example, it is well known that the transport in slabs deviates from diffusion when the sample thickness L is less than about 10 times the transport mean free path [57–59]. For heterogeneous systems, we anticipate that additional complications arise when the sizes of nonscattering regions are on the order of the sample size. This section therefore discusses the relation between transport in unbounded media, as treated in the preceding sections, and transport in finite-size media. We show that the theory of diffusion constants is not directly applicable to bounded systems when the size of heterogeneities is on the order of the system dimensions.

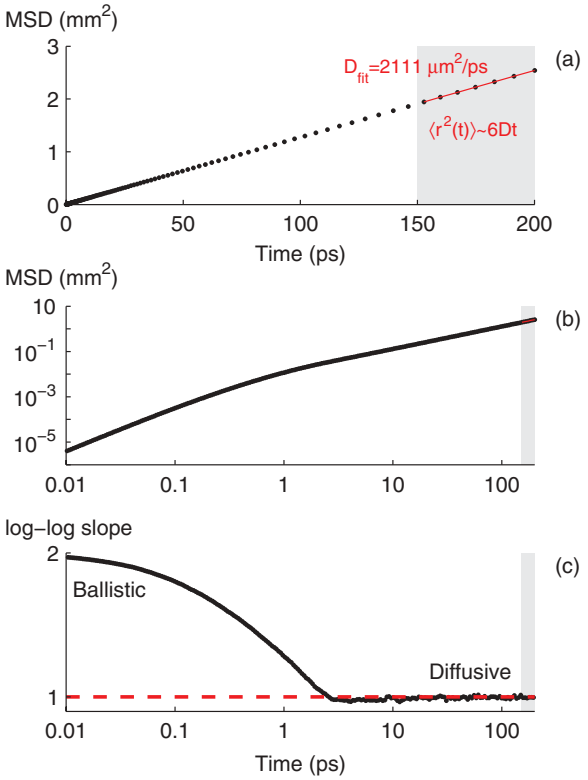

FIG. 7. (Color online) Transport dynamics for a holey system based on a fractal sphere packing (sphere radii ranging from 2.5 to 200 μm, each category occupying about 4% of the volume, the overall sphere filling fraction being $\phi = 0.7005$). Here the walker crosses on average one sphere between scattering events ($\ell_s = \bar{\Delta} = 5.89$ μm). The exact $E[S^2]$ as obtained from simulations would, if steps were independent, result in a diffusion constant of 2866 μm^2/ps (step data were presented in Fig. 6, but note that the exponential spacing model in this particular case overestimates the $E[S^2]/E[S]$ ratio by about 5%). In contrast, a linear fit over the temporal range indicated in gray in (a) gives $D = 2111 \pm 7$ μm^2/ps (mean $\pm$ standard error of the mean, as obtained from five simulation repetitions with 10^5 random walkers each). That the observed D is about 25% lower is clear evidence that step correlations play an important role.

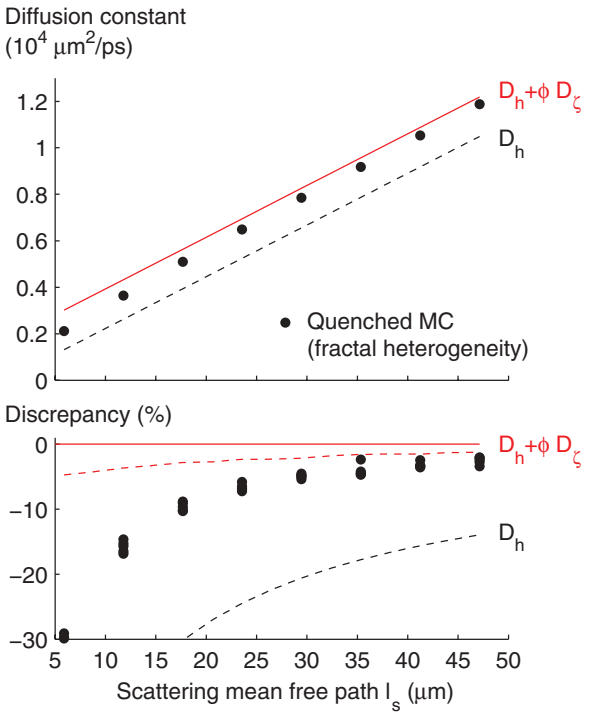

FIG. 8. (Color online) Also for strongly polydispersive systems, our probabilitisic theory is successful. The role of step correlations is, however, a complicated matter. In our particular fractal system, where 400-μm-diam spheres are the largest nonscattering regions, the role of correlation becomes small when ℓ_s is a few times larger than the mean void spacing $\bar{\Delta}$. At $\ell_s = 4\bar{\Delta} \approx 24$ μm, the asymptotic D obtained from MSD evolution is then only 4% lower than what the step statistics from quenched simulations tells us. The mean step $E[S] = \ell_h$ is then about 80 μm, a length that apparently is large enough to render the step anticorrelation related to the crossing of large spheres relatively small. Here it should be noted that the exponential spacing model overestimates $E[S^2]$ by a few percent (see the discussion in Fig. 6). The exact diffusion constant we would see if steps were independent can be estimated from the step statistics of simulations [via Eq. (7)] and is in this graph indicated by the dashed red line. Although the error caused by our model ($D_h + \phi D_\zeta$) is only a few percent, it is still important to realize that the step correlation is negligible when the actual diffusion constants (solid dots) meet the dashed line.

This issue of bounded heterogeneous systems is particularly relevant to the ongoing discussion of anomalous transport in Lévy glass [33–37,47,48]. Lévy glasses are turbid materials with strong (fractal) spatial heterogeneity in the density of scatterers. The heterogeneity is engineered and controlled by the embedding nonscattering regions that follow a power-law size distribution into a turbid medium. More specifically, the nonscattering regions are composed of glass spheres of sizes that are (ideally) exponentially sampled from the smallest radius $r_{\min}$ to the largest radius $r_{\max}$. Assuming one sphere crossing per step and a negligible contribution from the intersphere media, setting the number density of spheres $n \sim r^{-(\alpha+2)}$ should produce a step length distribution that falls off as $\ell^{-(\alpha+1)}$ [34]. On scales on the order of the maximal sphere size, as in slabs of thickness $L = 2r_{\max}$, the transport is then believed to be close to that of a Lévy walk. Although the probabilistic theory presented here represents a significant contribution to the topic of Lévy glass design, this falls outside the main focus of this article. A view of this specific but important matter is, nonetheless, given in Appendix B. Here we will instead stick to the more general question of the relation between transport in unbounded and bounded media.

The system studied in the preceding section is in fact an unbounded Lévy glass with $\alpha = 1$. Its composition closely resembles the Lévy glass systems that have been studied experimentally [33,48] and by simulation [37]. Our study shows that step correlations play an important role for transport in the unbounded systems and the resulting diffusion constant for the system is about 2.11×10^3 μm^2/ps. Looking back at Fig. 7 and the evolution of the mean-square displacement (MSD), it appears that the onset of diffusion occurs surprisingly early. The MSD starts to grow approximately linearly with time after 2 ps. At this time, the MSD is about 0.027 mm^2, meaning that the average walker displacement is (roughly) on the order of 150 μm. From this it may be

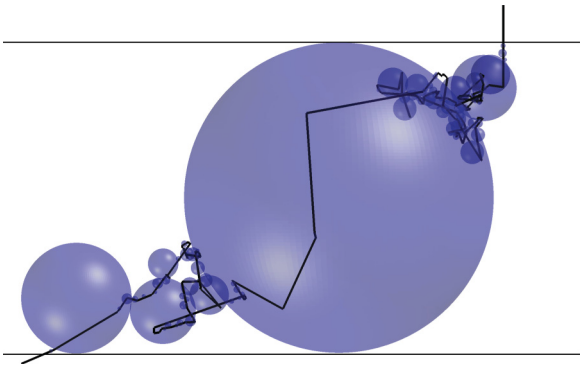

FIG. 9. (Color online) Two-dimensional projection of a simulated trajectory through a 3D Lévy glass slab. In this case, the random walker crosses one of the largest spheres. To obtain the average transmission properties, walkers are injected randomly on top of the slab (the slab consists of 9 507 676 spheres, the thickness being $L = 2r_{\max} + \epsilon = 402\ \mu\text{m}, \phi = 0.7005$). Analysis of the sphere packing reveals that the exponential spacing model applies equally well as in the unbounded case and that $\ell_s = \bar{\Delta} = 5.89\ \mu\text{m}$ indeed renders $E[N]$ very close to one.

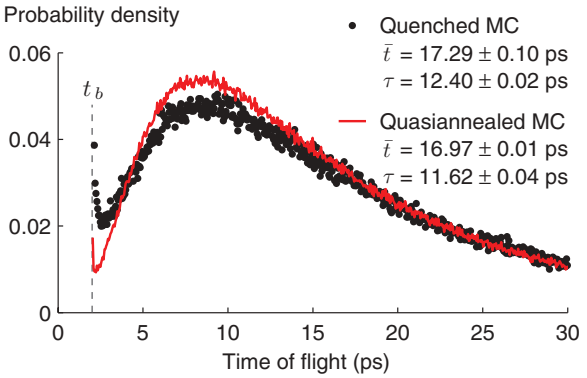

FIG. 10. (Color online) Transmission dynamics for a Lévy glass, i.e., a bounded fractal sphere packing (slab thickness $L = 402\ \mu\text{m}$, maximal sphere diameter 400 μm). Important characteristics such as mean transmission time $\bar{t}$ and decay constant τ show that the dynamics is not consistent with diffusion (see the main text). This conclusion is also supported by the significant amount of quasiballistic transmission (the truly ballistic component at $t_b = L/v$ is not part of the shown distribution). The dynamics is instead well reproduced by a quasiannealed simulation based on the exponential spacing model. This mutual agreement indicates that step correlations play a less important role here than in the unbounded case. Statistics are based on three and ten repetitions of 10^6 walkers for the quenched and quasiannealed simulations, respectively (mean times and the decay constant are stated in the graph as the mean ± standard error). The transmission in both cases is about 12%, while the the ballistic fraction of the transmission is 0.6% and 0.15% (higher in the quenched case).

tempting to conclude that transport is diffusive after some 150 μm and that the transmission through a Lévy glass of thickness $L = 2r_{\max} = 400\ \mu\text{m}$ indeed will be diffusive. In fact, Groth *et al.* [37] have claimed that transport through Lévy glass follows regular diffusion. To check whether the above reasoning is adequate or not and to investigate the claim of Groth *et al.*, we have performed simulations of the transport through a bounded version of this sphere packing.

Figure 9 illustrates our simulations of transport through bounded systems. Our conclusion from these simulations is that transport through Lévy glass cannot be described by diffusion. Along with a significant amount of ballistic and quasiballistic transmission, we observe major deviations from diffusion theory also in mean transmission time and the long-time decay constant (lifetime). Diffusion theory of light transport is well established and in the diffusive regime, for example, it is well known [60] that the mean transmission time $\bar{t}_D$ follows

$$\bar{t}_D = \frac{(L + 2z_e)^2}{6D} \tag{25}$$

and that the decay time constant τ_D is given by

$$\tau_D = \frac{(L + 2z_e)^2}{\pi^2 D} \tag{26}$$

In the above formulas, L denotes slab thickness and $z_e = \frac{2}{3}\ell_t$ is the so-called extrapolation length. If transport through the slab is diffusive with $D = 2111\ \mu\text{m}^2/\text{ps}$, macroscopic transport should be identical to a random walk of independent and exponentially distributed steps with average length $\ell_t = 3D/v \approx 31.7\ \mu\text{m}$. We would thus expected a mean transmission time of about $\bar{t}_D = 15.6$ ps and a decay constant of about $\tau_D = 9.5$ ps. In contrast, as shown in Fig. 10, quenched simulations result in a mean transmission time of 17.3 ps and decay constant of 12.4 ps. In fact, the observed combination of $\bar{t}$ and τ is not consistent with any diffusion constant. Furthermore, the significant amount of ballistic and quasiballistic light alone indicates that diffusion cannot capture the transport well. We therefore conclude that transport in Lévy glass is not governed by diffusion. Instead, we found that the dynamics is well reproduced by what we call a quasiannealed simulation in which we mimic the step distribution but effectively remove step anticorrelations. In this straightforward simulation, which is a numerical correspondent to our probabilistic theory, steps are generated on the basis of the exponential spacing model under the requirement that when the walker is about to a make a chord, this chord cannot be longer than the distance to the slab boundary (see Appendix C for a more detailed description). The step length is thus position and direction dependent, but step correlations are heavily suppressed. Although it is beyond the scope of this article to investigate this interesting result in detail, it appears as if the presence of boundaries in the quenched system strongly alters the role of step correlations.

IV. CONCLUSION

We have presented a probabilistic theory for transport in systems with a quenched heterogeneous distribution of scatterers. The focus was on random systems and via a simple model of the quenched disorder we have been able to derive analytical expressions for, notably, the mean step, the mean-square step, the diffusion constant, and void crossing probabilities. Here we repeat two key results. First, we have shown that the mean step is given by [Eq. (5)]

$$E[S] = \frac{\ell_s}{1 - \phi} = \ell_h$$

and thus equals the homogenized (exponential) scattering mean free path ℓ_h, being dependent only of void filling fraction ϕ, not its size and shape. Second, for holey systems in the form of random sphere packings we have also shown (in the limit of weak step correlations) that the asymptotic diffusion constant is [Eq. (23)]

$$D = \frac{1}{3}v\ell_h + \phi\frac{1}{6}v\frac{E[\zeta^2]}{E[\zeta]}.$$

In cases where step correlations are non-negligible, under the reasonable assumption that steps are not positively correlated, this expression can function as an upper bound on the diffusion constant. All our theoretical results are well supported by Monte Carlo simulations of random walks in holey systems based on random sphere packings. We have also shown that the relation between transport in unbounded and bounded system is particularly complex when heterogeneities are on the order of the system size (especially regarding the onset of regular diffusion and the role of step correlations).

Given the abundance of turbid materials where scatterers are not homogeneously distributed, we believe that both our viewpoint and our results can be of value for a wide range of topics, from fundamental work on light transport to applied spectroscopy of heterogeneous media such as biological tissues, food products, and powder compacts. In particular, viewing transport as a quenched holey random walk may turn out to be an important approach for work directed towards the understanding of the optics and spectroscopy of complex porous media with broad and/or anisotropic pore-size distribution, such as pharmaceutical tablets [29,61]. In this context, it should be noted that generalization of our work to systems with impedance mismatch and anisotropic heterogeneity should be rather straightforward. Accounting for refractive index mismatch, for example, is standard in the study of light transport [62,63]. Finally, as discussed earlier, a theoretical account of quenched systems with strong step correlations is more challenging, but equally important.

ACKNOWLEDGMENTS

This work benefited from the European Network of Excellence for Nanophotonics for Energy Efficiency and the ERC grant Photbots. T.S. gratefully acknowledge funding from The Swedish Research Council (postdoctoral fellowship Grant No. 2010-887). Erik Alerstam, Raffaella Burioni, and Alessandro Vezzani are thanked for useful discussions.

APPENDIX A: DERIVATIONS FOR $E[S^2]$

In this Appendix we provide a derivation of the expression for the mean-square step given in the main text. We start by expanding the mean-square step into three components

$$E[S^2] = E\left[S^2_{\text{turbid}}\right] + E\left[S^2_{\text{void}}\right] + 2E[S_{\text{turbid}}S_{\text{void}}]. \quad \text{(A1)}$$

Since $E[S^2_{\text{turbid}}] = 2\ell_s^2$ by definition, the challenge is the last two terms. As mentioned in the main text, we will make the important assumption that the length of the different chords involved in a step is independent of the number of spheres crossed (this means, e.g., that we assume that the spacing between two spheres is independent of the sizes of these spheres). By splitting the outcome of S_{void} into cases of different numbers of sphere crossings, we can calculate the two terms from the rules of total expectation values. Starting with $E[S^2_{\text{void}}]$, we have

$$\begin{aligned}
E\left[S^2_{\text{void}}\right] &= \sum_{n=0}^{\infty} P_n E\left[S^2_{\text{void}}|N=n\right] \\
&= \sum_{n=0}^{\infty} P_n E\left[\left(\sum_{i=0}^{n}\zeta_i\right)^2\right] \\
&= \sum_{n=0}^{\infty} P_n\{nE[\zeta^2] + n(n-1)E[\zeta]^2\} \\
&= E[N]E[\zeta^2] + (E[N^2] - E[N])E[\zeta]^2 \\
&= \phi\ell_h\frac{E[\zeta^2]}{E[\zeta]} + 2\frac{\ell_s^2}{\bar{\Delta}^2}E[\zeta]^2. \quad \text{(A2)}
\end{aligned}$$

When calculating $E[S_{\text{turbid}}S_{\text{void}}]$ we must remember that they are dependent variables. We can break this dependence by again splitting into cases of different numbers of sphere crossings

$$\begin{aligned}
E[S_{\text{turbid}}S_{\text{void}}] &= \sum_{i=0}^{\infty} P_n E[S_{\text{turbid}}S_{\text{void}}|N_{\text{cross}}=n] \\
&= \sum_{i=0}^{\infty} P_n n E[\zeta]E[S_{\text{turbid}}|N=n] \\
&= \sum_{i=0}^{\infty} P_n n E[\zeta](n+1)\frac{\bar{\Delta}\ell_s}{\bar{\Delta}+\ell_s} \\
&= E[\zeta]\frac{\bar{\Delta}\ell_s}{\bar{\Delta}+\ell_s}(E[N^2]+E[N]) \\
&= 2E[\zeta]\frac{\bar{\Delta}\ell_s}{\bar{\Delta}+\ell_s}(E[N]^2+E[N]) \\
&= 2E[\zeta]\frac{\bar{\Delta}\ell_s}{\bar{\Delta}+\ell_s}\left(\frac{\ell_s^2}{\bar{\Delta}^2}+\frac{\ell_s}{\bar{\Delta}}\right) \\
&= 2E[\zeta]\frac{\bar{\Delta}\ell_s}{\bar{\Delta}+\ell_s}\frac{\ell_s(\ell_s+\bar{\Delta})}{\bar{\Delta}^2} \\
&= 2E[\zeta]\frac{\ell_s^2}{\bar{\Delta}}. \quad \text{(A3)}
\end{aligned}$$

The step to reach the third line, involving a calculation of $E[S_{\text{turbid}}|N=n]$, deserves a comment. This term tells us the average intervoid path made given a certain number of crossings. Having n crossings is the same as knowing that the step was longer than a sum of n spacings, but that the step in the could not cross the $(n+1)$th spacing. This event can be written as

$$\sum_{i=1}^{n}\Delta_i < S_{\text{turbid}} < \left(\sum_{i=1}^{n}\Delta_i\right) + \Delta_{n+1}. \quad \text{(A4)}$$

Noting that the sum of the n spacing is an Erlang distribution (sum of n independent exponential distributions), we can calculate $E[S_{\text{turbid}}|N=n]$ by doing three-dimensional integration over the joint distribution of three random variables [the Erlang distribution, $\Delta_{n+1} \in \exp(\bar{\Delta})$, and $S_{\text{turbid}} \in \exp(\ell_s)$].

The conditional expectation value is reached by integrating over the space corresponding to the event $N = n$, as expressed in Eq. (A4) (note that the joint density function must be renormalized by the probability of the event). The result is essentially the Γ function integral. A more elegant way to solve the problem, however, is to see the problem as an encounter of spacings Δ_i, where the memoryless nature of the random process makes it possible to treat each crossing independently. If a walker manages to cross a certain spacing, the best estimate of the spacing crossed is $E[\Delta|S_{\text{turbid}} > \Delta]$. In contrast, when the walker finally does *not* manage to cross a spacing, the step made in this last part (after the last void crossing) is on average $E[S_{\text{turbid}}|\Delta > S_{\text{turbid}}]$. These two terms can be calculated by means of a two-dimensional integral over their joint probability density function (the symmetry of the problem makes one term follow from the other)

$$E[\Delta|S_{\text{turbid}} > \Delta] = \frac{\iiint_{\ell>\delta} \delta p(\ell,\delta) d\ell\, d\delta}{\iiint_{\ell>\delta} p(\ell,\delta)\ell\, d\delta} = \frac{\bar{\Delta}\ell_s}{\bar{\Delta}+\ell_s} = E[S_{\text{turbid}}|\Delta > S_{\text{turbid}}]. \tag{A5}$$

Thus, when a walker manages to cross an intersphere spacing, that spacing is on average $E[\Delta|S_{\text{turbid}} > \Delta]$. As emphasized above, the memoryless nature of the exponential distribution allows us to forget the total intersphere step already made and make the same conclusion after each crossing. When the walker finally fails to cross a spacing, the average step taken after the last void crossing was $E[S_{\text{turbid}}|\Delta > S_{\text{turbid}}]$. Given that there were n crossings in total, the expected path is therefore

$$E[S_{\text{turbid}}|N = n] = nE[\Delta|S_{\text{turbid}} > \Delta] + E[S|\Delta > S_{\text{turbid}}] = (n+1)\frac{\bar{\Delta}\ell_s}{\bar{\Delta}+\ell_s}. \tag{A6}$$

We reach the expression (20) by summing the three contributions and reducing the quadratic polynomial

$$\begin{aligned} E[S^2] &= E\left[S^2_{\text{turbid}}\right] + E\left[S^2_{\text{void}}\right] + 2E[S_{\text{turbid}}S_{\text{void}}] \\ &= 2\ell_s^2 + \phi\ell_h\frac{E[\zeta^2]}{E[\zeta]} + 2\frac{\ell_s^2}{\bar{\Delta}^2}E[\zeta]^2 + 4E[\zeta]\frac{\ell_s^2}{\bar{\Delta}} \\ &= 2\ell_s^2\left(1+\frac{E[\zeta]}{\bar{\Delta}}\right)^2 + \phi\ell_h\frac{E[\zeta^2]}{E[\zeta]} \\ &= 2\ell_s^2\left(1+\frac{\phi}{1-\phi}\right)^2 + \phi\ell_h\frac{E[\zeta^2]}{E[\zeta]} \\ &= 2\ell_h^2 + \phi\ell_h\frac{E[\zeta^2]}{E[\zeta]}. \end{aligned} \tag{A7}$$

APPENDIX B: LÉVY GLASS DESIGN

When Lévy glasses were introduced by Barthelemy *et al.* [33], the scatterer concentration was selected aiming at achieving, on average, one scattering event between sphere crossings (i.e., $E[N] = 1$, where N denotes the number of sphere crossings in a step). The design principle was not elaborated in more detail and exactly how the filling fraction and scattering strength affect crossings statistics was not known. The intersphere transport mean free path was in fact chosen to match the smallest sphere diameter, i.e., $\ell_t = 2r_{\text{min}} = 5\ \mu$m. The probabilistic theory presented in this work allows a selection of the scattering strength that more strictly fulfills the ideal Lévy glass design criteria. From Eq. (17) we see that $E[N] = 1$ is reached when $\ell_s = \bar{\Delta}$. As can be seen in Fig. 6, this result is confirmed by our simulations. In this respect [using Eq. (19) to express $\bar{\Delta}$], the ideal scattering strength is therefore

$$\ell_s^{\text{ideal}} = \bar{\Delta} = \frac{1-\phi}{\phi}E[\zeta]. \tag{B1}$$

Returning to the experimental work in Ref. [33], the filling fraction, as can be calculated from recipe given in the supplemental information therein, was about 67%. Via calculation of the mean chord, we find that the ideal ℓ_s for the samples used to investigate transmission scaling ranges from 9.5 μm ($L = 550\ \mu$m, $L = 2r_{\text{max}}$ being the Lévy glass slab thickness) to 4.2 μm ($L = 50\ \mu$m). Although the utilized scattering strength clearly is of the right order of magnitude, setting $\ell_s = 2r_{\text{min}}$ is not universally ideal. That the ideal ℓ_s varies with Lévy glass thickness is related to the fact that thicker samples include the use of larger spheres that fill space more efficiently than smaller ones. If the filling fraction ϕ is kept constant, the average sphere spacing will therefore increase with thickness. It is thus important to realize that studies of a series of Lévy glass with varying $L = 2r_i$ but with constant ϕ and ℓ_s come with an inherent mismatch with the ideal Lévy glass design principle. The implication this finding has on the design of scaling experiments remains to be elaborated. For completeness, it should also be noted that scattering is not fully isotropic in the discussed experiments. The titanium dioxide nanoparticles used give an anisotropy factor of $g \approx 0.6$, meaning that $\ell_s = (1-g)\ell_t \neq \ell_t$. This is an additional aspect that should be considered in the future.

In a more recent experimental paper, Burresi *et al.* [48] reported on weak localization of light (coherent backscattering) in Lévy glass. Therein samples had a filling fraction of about 70% and were manufactured using spheres of sizes from $r_{\text{min}} = 2.5\ \mu$m up to $r_{\text{max}} = 115\ \mu$m ($L \approx 230\ \mu$m). Our theory shows that the ideal ℓ_s is around 6.3 and 3.8 μm for the studied $\alpha = 1$ and 1.5 samples, respectively. In the article, reference experiments where scatterers were dispersed homogeneously rendered $\ell_t = 19\ \mu$m, indicating that the intersphere scattering strength was $l_t = 19/(1-\phi) = 5.7\ \mu$m. The experiments done were thus in close agreement with the ideal design principle (again, disregarding that scattering was anisotropic with $g = 0.6$).

Finally, a recent paper by Groth *et al.* [37] investigated transmission scaling in Lévy glasses via simulations of random walks in sphere packings. Therein simulations were stated to run with $\ell_s = r_{\text{min}}/2$ and it was said that this choice was made to ensure that "there is, on average, one scattering event between leaving and entering a sphere" (i.e., to ensure $E[N = 1]$). Given the findings of our present work, we believe that this level of scattering is too strong to render $E[N] = 1$ (at least for relevant filling fractions). Above we reported that experimental Lévy glass systems have had a filling fraction of about 70% and the ideal scattering mean free path always is significantly larger than the radius of the smallest sphere. Assuming that

Groth *et al*. were not studying very different systems, we believe that using $\ell_s = r_{\min}/2$ brings them far from the ideal situation where $E[N] = 1$. However, since the utilized filling fractions were not stated, we cannot be fully quantitative. Nonetheless, it is important to note that while setting ℓ_s very small will take us close to the desired $\ell^{-(\alpha+1)}$ power-law decay in the step length distribution [multiple crossings getting increasingly unlikely, i.e., $P(N > 1)$ negligible], such a procedure will induce strong step correlations that affect transport.

APPENDIX C: QUASIANNEALED RANDOM WALK

The proposed quasiannealed random walk aims at mimicking the step length distribution of the quenched system while removing step correlations related to the quenched disorder. After random walker initiation and each scattering event, a random step $S_{\text{turbid}} \in \exp(\ell_s)$ to be traveled through the turbid component is generated. The length of this step is first compared to the distance to the boundary Δ_b along the current direction of propagation. If $S_{\text{turbid}} > \Delta_b$, the walker leaves the sample and a transmission or reflection time is registered. If, in contrast, $S_{\text{turbid}} < \Delta_b$, S_{turbid} is instead compared to a randomly generated exponential distributed distance to the closest virtual sphere $\Delta_s \in \exp(\bar{\Delta})$ (cf. the exponential spacing model described in Sec. II D). If $S_{\text{turbid}} < \Delta_s$, scattering will take place and the procedure will start over when a new direction and a new step S_{turbid} have been generated. If $S_{\text{turbid}} > \Delta_s$, the walker will cross a nonscattering region, after which the remaining part of the step $S_{\text{turbid}} - \Delta_s$ will be used as the new step forward (to be compared with the updated Δ_b and a new sphere spacing). The length traveled through the void (a random chord ζ) is generated based on the distribution of chords predicted by equilibrium considerations, i.e., the density function given in Eq. (12). The related cumulative distribution functions (CDFs) are

$$F_\zeta(x) = P(\zeta \leqslant x) = 1 - P(\zeta > x) \tag{C1}$$

$$= 1 - \sum_{i:2r_i>x} \int_x^{2r_i} p_i \frac{x}{2r_i^2}\, dx \tag{C2}$$

$$= 1 - \sum_{i:2r_i>x} p_i \left(1 - \frac{x^2}{4r_i^2}\right) \tag{C3}$$

$$= 1 - \sum_{i:2r_i>x} p_i + \sum_{i:2r_i>x} p_i \frac{x^2}{4r_i^2}. \tag{C4}$$

Solving $y = F_\zeta(x)$, we find

$$x = F_\zeta^{-1}(y) = \sqrt{\frac{y - 1 + \sum_{i:F(2r_i)>y} p_i}{\sum_{i:F(2r_i)>y} \frac{p_i}{4r_i^2}}}. \tag{C5}$$

We use this inverse CDF to generate the random chord length ζ, setting

$$\zeta = F_\zeta^{-1}(U), \tag{C6}$$

where U is a random variable uniformly distributed in $[0,1]$. Note that a generated chord is accepted only if it is smaller than the current distance to the boundary. If a generated chord is larger than the distance to the boundary it is discarded and the generation is remade. This means that long steps to some extent are underrepresented compared to the equilibrium consideration that lies behind the chord length distribution. At this stage, it cannot be ruled out that this has some impact on quantities such as mean transit time and decay rate (lifetime). The role of step correlations in transport through quenched disorder certainly deserves further attention in the future.

[1] G. Thomas and K. Stamnes, *Radiative Transfer in the Atmosphere and Ocean* (Cambridge University Press, Cambridge, 2002).

[2] M. I. Mishchenko, L. D. Travis, and A. A. Lacis, *Multiple Scattering of Light by Particles: Radiative Transfer and Coherent Backscattering* (Cambridge University Press, Cambridge, 2006).

[3] A. B. Davis and A. Marshak, Rep. Prog. Phys. **73**, 026801 (2010).

[4] V. V. Tuchin, *Tissue Optics: Light Scattering Methods and Instruments for Medical Diagnosis*, 2nd ed. (SPIE, Bellingham, WA, 2007).

[5] A. J. Welch and M. J. C. Gemert, *Optical-Thermal Response of Laser-Irradiated Tissue* (Springer, Berlin, 2010).

[6] L. V. Wang and H.-i. Wu, *Biomedical Optics: Principles and Imaging* (Wiley, New York, 2007).

[7] B. J. Berne and R. Pecora, *Dynamic Light Scattering: With Applications to Chemistry, Biology, and Physics* (Dover, New York, 2000).

[8] G. Reich, Adv. Drug Delivery Rev. **57**, 1109 (2005).

[9] H. W. Siesler, Y. Ozaki, S. Kawata, and H. M. Heise, *Near-Infrared Spectroscopy: Principles, Instruments, Applications* (Wiley, New York, 2008).

[10] Z. Shi and C. A. Anderson, J. Pharm. Sci. **99**, 4766 (2010).

[11] A. Liemert and A. Kienle, Phys. Rev. A **83**, 015804 (2011).

[12] A. Ishimaru, *Wave Propagation and Scattering in Random Media* (Academic, New York, 1978).

[13] A. Lagendijk and B. A. van Tiggelen, Phys. Rep. **270**, 143 (1996).

[14] R. Pierrat, L. J. Greffet, and R. Carminati, J. Opt. Soc. Am. A **23**, 1106 (2006).

[15] S. Lovejoy, A. Davis, P. Gabriel, D. Schertzer, and G. L. Austin, J. Geophys. Res. **95**, 11699 (1990).

[16] A. B. Davis, A. Marshak, and K. P. Pfeilsticker, *Proceedings of the Ninth Atmospheric Radiation Measurement Science Team Meeting, San Antonio, 1999* (US DOE, Washington, DC, 1999).

[17] T. Scholl, K. Pfeilsticker, A. B. Davis, H. Klein Baltink, S. Crewell, U. Löhnert, C. Simmer, J. Meywerk, and M. Quante, J. Geophys. Res. **111**, D12211 (2006).

[18] H. Liu, B. Chance, A. H. Hielscher, S. L. Jacques, and F. K. Tittel, Med. Phys. **22**, 1209 (1995).

[19] M. Firbank, S. R. Arridge, M. Schweiger, and D. T. Delpy, Phys. Med. Biol. **41**, 767 (1996).

[20] A. H. Hielscher, R. E. Alcouffe, and R. L. Barbour, Phys. Med. Biol. **43**, 1285 (1998).
[21] D. A. Boas, J. P. Culver, J. J. Stott, and A. K. Dunn, Opt. Express **10**, 159 (2002).
[22] G. Bal, J. Comput. Phys. **180**, 659 (2002).
[23] N. Shah, A. E. Cerussi, D. Jakubowski, D. Hsiang, J. Butler, and B. J. Tromberg, J. Biomed. Opt. **9**, 534 (2004).
[24] A. P. Gibson, J. C. Hebden, and S. R. Arridge, Phys. Med. Biol. **50**, R1 (2005).
[25] V. Ntziachristos, J. Ripoll, L. V. Wang, and R. Weissleder, Nat. Biotechnol. **23**, 313 (2005).
[26] T. Svensson, S. Andersson-Engels, M. Einarsdóttír, and K. Svanberg, J. Biomed. Opt. **12**, 014022 (2007).
[27] A. Dogariu, J. Uozumi, and T. Asakura, Waves Random Media **2**, 259 (1992).
[28] C. M. Sorensen, Aerosol Sci. Technol. **35**, 648 (2001).
[29] E. Alerstam and T. Svensson, Phys. Rev. E **85**, 040301 (2012).
[30] D. J. Durian, D. A. Weitz, and D. J. Pine, Science **252**, 686 (1991).
[31] A. S. Gittings, R. Bandyopadhyay, and D. J. Durian, Europhys. Lett. **65**, 414 (2004).
[32] A. Davis and A. Marshak, *in Fractal Frontiers*, edited by M. M. Novak and T. G. Dewey (World Scientific, Singapore, 1997), pp. 63–72.
[33] P. Barthelemy, J. Bertolotti, and D. S. Wiersma, Nature (London) **453**, 495 (2008).
[34] J. Bertolotti, K. Vynck, L. Pattelli, P. Barthelemy, S. Lepri, and D. S. Wiersma, Adv. Funct. Mater. **20**, 965 (2010).
[35] P. Barthelemy, J. Bertolotti, K. Vynck, S. Lepri, and D. S. Wiersma, Phys. Rev. E **82**, 011101 (2010).
[36] P. Buonsante, R. Burioni, and A. Vezzani, Phys. Rev. E **84**, 021105 (2011).
[37] C. W. Groth, A. R. Akhmerov, and C. W. J. Beenakker, Phys. Rev. E **85**, 021138 (2012).
[38] A. B. Kostinski, J. Opt. Soc. Am. A **18**, 1929 (2001).
[39] R. A. Shaw, A. B. Kostinski, and D. D. Lanterman, J. Quant. Spectrosc. Radiat. Transfer **75**, 13 (2002).
[40] A. B. Davis and A. Marshak, J. Quant. Spectrosc. Radiat. Transfer **84**, 3 (2004).
[41] M. Frank and T. Goudon, Kinet. Relat. Models **3**, 395 (2010).
[42] E. W. Larsen and R. Vasques, J. Quant. Spectrosc. Radiat. Transfer **112**, 619 (2011).
[43] A. B. Davis and M. B. Mineev-Weinstein, J. Quant. Spectrosc. Radiat. Transfer **112**, 632 (2011).
[44] G. Bal and W. Jing, J. Quant. Spectrosc. Radiat. Transfer **112**, 660 (2011).
[45] D. J. Behrens, Proc. Phys. Soc. London Sect. A **62**, 607 (1949).
[46] J. Lieberoth and A. Stojadinović, Nucl. Sci. Eng. **76**, 336 (1980).
[47] R. Burioni, L. Caniparoli, and A. Vezzani, Phys. Rev. E **81**, 060101 (2010).
[48] M. Burresi, V. Radhalakshmi, R. Savo, J. Bertolotti, K. Vynck, and D. S. Wiersma, Phys. Rev. Lett. **108**, 110604 (2012).
[49] M. C. W. van Rossum and T. M. Nieuwenhuizen, Rev. Mod. Phys. **71**, 313 (1999).
[50] J.-P. Bouchaud and A. Georges, Phys. Rep. **195**, 127 (1990).
[51] D. ben Avraham and S. Havlin, *Diffusion and Reactions in Fractals and Disordered Systems* (Cambridge University Press, Cambridge, 2000).
[52] G. L. Olson, D. S. Miller, E. W. Larsen, and J. E. Morel, J. Quant. Spectrosc. Radiat. Transfer **101**, 269 (2006).
[53] W. J. M. De Kruijf and J. L. Kloosterman, Ann. Nucl. Energy **30**, 549 (2003).
[54] S. Torquato and B. Lu, Phys. Rev. E **47**, 2950 (1993).
[55] D. Guéron and A. Mazzolo, Phys. Rev. E **68**, 066117 (2003).
[56] S. Torquato, *Random Heterogeneous Materials: Microstructure and Macroscopic Properties* (Springer, Berlin, 2001).
[57] K. M. Yoo, F. Liu, and R. R. Alfano, Phys. Rev. Lett. **64**, 2647 (1990).
[58] R. H. J. Kop, P. de Vries, R. Sprik, and A. Lagendijk, Phys. Rev. Lett. **79**, 4369 (1997).
[59] R. Elaloufi, R. Carminati, and J.-J. Greffet, J. Opt. Soc. Am. A **21**, 1430 (2004).
[60] I. M. Vellekoop, P. Lodahl, and A. Lagendijk, Phys. Rev. E **71**, 056604 (2005).
[61] T. Svensson, E. Alerstam, J. Johansson, and S. Andersson-Engels, Opt. Lett. **35**, 1740 (2010).
[62] L. Wang, S. L. Jacques, and L. Zheng, Comput. Meth. Prog. Bio. **47**, 131 (1995).
[63] Z. Sadjadi and M. F. Miri, Phys. Rev. E **84**, 051305 (2011).